Disruption of surface-induced smectic order by periodic surface corrugations

Ghanshyam P. Sinha* and Charles Rosenblatt
Department of Physics, Case Western Reserve University, Cleveland, Ohio 44106-7079

Leonid V. Mirantsev
Institute for Problems of Mechanical Engineering, Academy of Sciences of Russia, St. Petersburg, 199178, Russia

(Received 17 July 2001; revised manuscript received 17 December 2001; published 11 April 2002)

A Fréedericksz transition measurement is reported for a liquid crystal cell composed of surfactant-coated substrates. One substrate was locally scribed with the stylus of an atomic force microscope to create a nanoscopic grooved structure. The Fréedericksz threshold voltage was found to be smaller in the scribed region than in the unscribed region, indicating that the corrugated surface disrupts surface-induced smectic order, and that the effect grows toward the nematic–smectic-*A* transition temperature T_{NA} in conjunction with the smectic correlation length.

DOI: 10.1103/PhysRevE.65.041718 PACS number(s): 61.30.Gd

Interfacial effects in liquid crystals has long been a subject of interest from both the fundamental and applied perspectives [1]. It is well known [1–3] that for a substrate prepared for homeotropic order, smectic layering of a characteristic length scale ξ_c, comparable to the smectic correlation length ξ, may be induced at a smooth interface. Early on, experiments that probe this interfacial smectic layering involved a free surface, i.e., a liquid-crystal–air interface. Performing a nonperturbative small angle x-ray reflectivity measurement, Als-Nielsen *et al.* [4] demonstrated the existence of smectic order at the free surface of octyloxy cyanobiphenyl (8OCB), in both the nematic and isotropic phases. More recently Mol *et al.* examined layer-by-layer thinning in a free standing film above the nematic–smectic-*A* phase transition [5]. For experiments at a solid substrate, Ocko studied layer-by-layer growth at the first order isotropic–smectic-*A* transition [3]. He demonstrated that smectic layer formation tends to become less discrete as the isotropic–nematic–smectic-*A* triple point is approached for shorter mesogens of the alkylcyanobiphenyl homologous series. Experiments at a substrate may be difficult, however, because of the necessity of obtaining a molecularly smooth surface. Ocko, for example, was unable to completely rule out a small amount of penetration (a few angstroms) of the liquid crystal molecules into the alkyl coating at the substrate [3]. Thus, for a variety of practical reasons there is not an extensive literature that deals with smectic ordering at a substrate, particularly at the second order nematic–smectic-*A* transition temperature T_{NA}.

In principle, the origin of substrate-induced smectic order could be similar to that at a free surface, but with some important differences. For example, at a substrate there is a direct interaction between the substrate material and the liquid crystal, promoting smectic order at the interface. On the other hand, the surface chemical compositon and topography may retard the growth of surface-induced smectic ordering. An experimental result that demonstrates the promotion of substrate-induced smectic order in the nematic phase was performed by Rosenblatt [6], in which he observed an anomalous increase in the Fréedericksz transition threshold of a nematic cell due to the growth of difficult-to-deform smectic layers at the two substrates. Qualitatively, for a cell of thickness l, the effective thickness of the deformable nematic region is approximately $l_U = l - 2\xi_c$, and the resulting magnetic Fréedericksz threshold is approximately $H_{th} \simeq \pi(K_{33}/\Delta\chi_M)^{1/2}/l_U$, where K_{33} is the bend elastic constant and $\Delta\chi_M$ is the magnetic susceptibility anisotropy. Note that the exact solution is considerably more complicated [6], as the smectic order parameter varies spatially into the bulk of the cell, with a concommitant spatial variation of the tilt susceptibility of the director. Despite the idealized case of very flat substrates, however, in most practical situations liquid crystals interact with solid substrates whose surfaces possess a small degree of corrugation. Recently, Mirantsev showed theoretically [7,8] that the presence of a one-dimensional sinusoidal surface microrelief with a period of 1 μm and an amplitude of order 30 nm results in a deformation of the surface-induced smectic layers. This in turn leads to the suppression of the interfacial smectic-*A* structure. Based on Refs. [7] and [8], we would expect that a surface microrelief at one substrate would give rise to an effective thickness l_R for the deformable region of a nematic cell that is *greater* than l_U, the deformable region of a cell of the same thickness but with two flat surfaces, i.e., $l_R = l - \xi_c - \xi_c' > l_U$. Here ξ_c' is the characteristic penetration depth of the (partially) disrupted smectic layers at the corrugated surface, and is less than or equal to ξ_c (which in principle diverges on approaching T_{NA}). In this paper we report on measurements of the Fréedericksz threshold field in the nematic phase in a homeotropically aligned cell on cooling toward the nematic–smectic-*A* phase transition. The cell contains two regions: The first region has two near-perfectly flat substrate surfaces and the (adjacent) second region has a corrugated substrate. Our results provide information about the effects of surface microrelief on surface-induced smectic order.

To achieve homeotropic alignment, an indium-tin-oxide (ITO) -coated glass substrate was first spin-coated with the homeotropic-alignment-promoting polyimide SE-1211 (Nis-

*Present address: Laboratorium voor Akoestiek en Thermische Fysica, KU Leuven, Celestijnenlaan, Belgium.

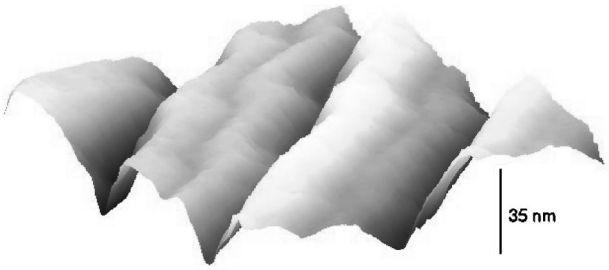

FIG. 1. Typical AFM rubbing of HTAB-coated substrate. The grooves are 200 nm apart and the average depth of the grooves is 22 nm.

san Chemicals) in order to provide a good wetting surface for the surfactant. A 0.2 wt % solution of hexadecyltrimethylammonium bromide (HTAB) in ethanol was then spin-coated onto the polyimide, and the ethanol was allowed to evaporate. This procedure provided a smooth surface (rms roughness $\lesssim 0.7$ nm) over most of the substrate for homeotropic alignment of the liquid crystal. As an aside, we note that direct spin coating of the HTAB/ethanol mixture onto the ITO resulted in randomly located pillars of surfactant which tended to break the stylus of the atomic force microscope (AFM) during the scribing process. To circumvent this problem the intermediate polyimide layer was added, which prevented formation of these pillars. In order to obtain a one-dimensional periodic corrugated surface, the stylus of the AFM was scanned in ''contact mode'' over an area of 100 μm$\times$100 μm. This facilitated a comparison between measurements of the threshold fields for flat and corrugated regions in close proximity, which helped to avoid two possible uncertainties—temperature gradients across the cell and differences of cell thickness due to a deviation from parallelism of the top and bottom glass slides. The force between the stylus and the substrate surface determined the groove depth into the surfactant, while the periodicity of grooves was easily controlled by the AFM instrumentation. Experiments were performed for a number of cells having typical groove depths of order 25 nm, with spacings between the grooves of 200–250 nm. A typical relief created by scanning the surface in contact mode is shown in Fig. 1, where the image was obtained by rescanning the same area in noncontact mode. Cells were constructed from two glass plates, one with the AFM-rubbed area and the other plate completely unrubbed, by using Mylar spacers and adjusting for optimum parallelism. The thickness was measured using an interferometric scheme [9] and was found to be 3.4 ± 0.1 μm in each case. The cells were filled with a racemic mixture of the negative dielectric anisotropy liquid crystal SCE12R (Merck), thus facilitating a bend deformation in a homeotropic cell when subjected to an electric field above the Fréedericksz threshold. (This material has a wide nematic temperature region below which there is a smectic-*A* phase followed by a smectic-*C* phase.) Since the area of the grooved region was very small, the electric-field-based Fréedericksz transition measurements were performed in the following way. The cells were housed in an oven that was temperature controlled to approximately ±5 mK and illuminated with polarized

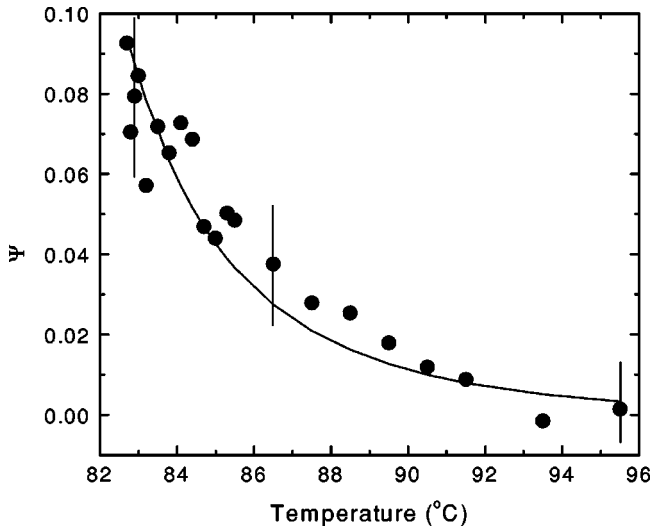

FIG. 2. The dimensionless quantity Ψ versus temperature for a thin cell, where the maximum depth is 22 nm and the separation between grooves is 200 nm. Note that for $T<T_{NA}+0.7\,^{\circ}$C, the Fréedericksz transition is first order. The solid line is the fit to theory.

light from an argon-ion laser at wavelength $\lambda=488$ nm and chopped at frequency $\nu=317$ Hz. A lens of focal length $f=2.5$ cm was placed downstream at a distance slightly larger than its focal length. The light then passed through an analyzer, and a real image of the sample was formed a distance of 250 cm from the lens; the overall magnification factor was $M\approx100$. A photodiode detector having an active area of approximately 1 mm^2 detected the light passing through the rubbed square. One end of a multimode optical fiber was placed just outside the image of this square and the other end was fed into a matching photodiode detector. By using a fiber we were able to circumvent the combined bulk of both detector housings and measure the liquid crystal sample at two points corresponding to a separation in the sample of 150 μm, thereby minimizing artifacts due to temperature gradients. The outputs from the two detectors were fed into two lock-in amplifiers that were referenced to the chopping frequency. A 10 kHz voltage whose amplitude was ramped at 2 V min^{-1} was applied across the cell thickness by means of the ITO electrodes, and the signals on the lock-in amplifiers were computer recorded. The threshold voltages V_{th} in each of the two regions were determined by sharp increases in the intensity of light. Measurements were performed as a function of temperature on approaching T_{NA} from above.

If we define Ψ as the fractional increase of the threshold field in the unrubbed (flat) region over that of the rubbed (corrugated) region, we have

$$\Psi\equiv E_{th}^{U}/E_{th}^{R}-1, \tag{1}$$

where E_{th}^{U} is the threshold field in the unrubbed (flat) region and E_{th}^{R} is the threshold field in the rubbed (corrugated) region. Ψ, which was referred to as Φ in Ref. [6], is expected to grow with the smectic-*A* correlation length on cooling. In Fig. 2 the circles represent measured values of Ψ above T_{NA}

for a sample having grooves of depth 22 ± 4 nm spaced 200 nm apart. Measurements from other cells showed results consistent with Fig. 2, within experimental error bars as shown in the figure. The relatively large magnitude of the experimental error, which is comparable to that in Ref. [6], reflects the very small differences in threshold voltages between the two regions, as well as a small amount of unavoidable rounding of the intensity vs voltage data in the AFM-rubbed region. The rounding is due, in part, to the absence of a preferrred tilt direction for the negative dielectric anisotropy liquid crystal. A second order transition temperature $T_{NA}=82.0\,^{\circ}\mathrm{C}$ was determined to within 50 mK by observing the rapid shrinkage of disclinations around dust particles in the sample as the liquid crystal cooled into the smectic-*A* phase. In the region $T_{NA}<T\lesssim T_{NA}+0.7$ K we observed a Fréedericksz transition defined by a sharp front that moved across the sample with increasing applied field. We believe this to be a first order Fréedericksz transition, which originally was investigated with pairs of fields, i.e., a driving and a bias field [10–13]. Recently, Shi and Yue showed theoretically that a first order Fréedericksz transition may also occur with a single field, as long as both K_{11}/K_{33} and the sample thickness are small [14]; this is the case for our experiment close to T_{NA}. We therefore do not consider the data in this temperature region in our analysis below. In the region $T\gtrsim T_{NA}+0.7$ K the Fréedericksz transition appears to be of the usual second order variety, with the optical intensity rising smoothly from zero above the threshold field. Far above T_{NA} we find that Ψ is close to zero, indicating that the differences in the threshold field near T_{NA} are due to differences in surface-induced smectic ordering rather than to a difference in the anchoring energy between the rubbed and unrubbed regions.

Mirantsev has examined this problem theoretically using a de Gennes–type free energy [7,8], accounting for the profile of the smectic order parameter $\sigma(z)$ through the cell, including the smectic order parameter σ_0 at the interface. For the corrugation profile used in this experiment, Refs. [7] and [8] predict that smectic order is suppressed completely at the grooved substrate, i.e., $\xi_c'=0$. Thus, only one substrate—the flat substrate—contributes to the thinning of the deformable nematic region. The free energy for the liquid crystal is given by

$$F=\int_0^{l/2}\left[K_{33}(d\theta/dz)^2-\frac{\Delta\varepsilon}{4\pi}E^2\theta^2+D(z)\theta^2\right]dz, \qquad (2)$$

where $\Delta\varepsilon$ is the dielectric anisotropy and the third term is the energy required to tilt the director by an angle θ relative to the layer normal in a smectic-*A* phase. In a de Gennes model $D(z)=D_0\sigma^2$ [6], where D_0 is the inverse susceptibility for director tilt with respect to the smectic layer normal. We note that according to de Gennes [15] the bend elastic constant K_{33} diverges on approaching T_{NA} as

$$K_{33}=K_{33}^0+(k_BT/6)(\pi\xi(t)a^2). \qquad (3)$$

The term K_{33}^0 is the background part of $K_{33}(T)$ and the second term is the divergent part proportional to the smectic correlation length $\xi(t)=\xi_0t^{-\nu}$, where ξ_0 is the bare correlation length, the reduced temperature $t=(T-T_{NA})/T_{NA}$, ν is the associated critical exponent, T is temperature, k_B is Boltzmann's constant, and a is the molecular length. In order to apply Eq. (2) to our experiment, we first measured K_{33} and fitted that data to obtain ξ_0, T_{NA}, and ν. These results, in turn, were applied to the form for $D(z)$ in Eq. (2), allowing us to fit our Fréedericksz transition data for the corrugated surface with three additional material parameters r_0, C^*, and D_0 implicit in $D(z)$ and described in Refs. [7] and [8].

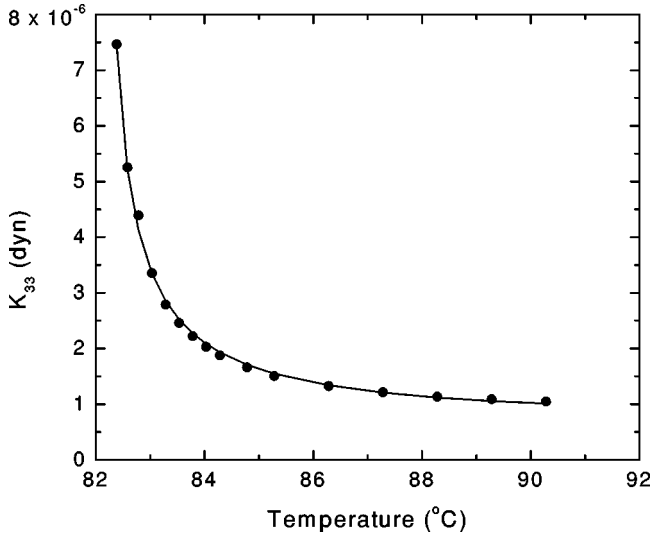

FIG. 3. K_{33} vs temperature for racemic mixture SCE12R. The solid line is a fit according to Eq. (3).

We measured K_{33} by inducing a Fréedericksz transition in a *thick* cell (thickness 58.6 μm), such that surface-induced smectic order plays virtually no role in the transition. Experimentally, light from a He-Ne laser passed through the sample, which was placed between an analyzer and a polarizer. The intensity of light was nearly zero below E_{th} and was monitored as a function of applied voltage across the cell. The Fréedericksz transition occurs at a critical field $E_{th}=\pi(4\pi K_{33}/\Delta\varepsilon)^{1/2}/l$. To obtain $\Delta\varepsilon$, the real part of the dielectric permittivity was measured for planar (thickness 14.6 μm) and homeotropic cells (thickness 14.6 μm) at 1 kHz using a high precision Andeen-Hagerling model 2500 capacitance bridge with a probe voltage of 0.15 V. The circles in Fig. 3 show the extracted values of K_{33} for the racemic mixture SCE12R. The fit gives $\nu=0.9\pm0.1$, $\xi_0=0.53\pm0.10$ nm, and $T_{NA}=82.00\pm0.05\,^{\circ}\mathrm{C}$, where a was taken as 30 Å. The value of ν, although larger than expected, seems to be consistent with the trend in which materials having smaller values of T_{NA}/T_{NI} have larger values of the exponent [16]. Here T_{NI} is the nematic-isotropic transition temperature. The value of the bare correlation length is also close to the reported value 0.45 nm from a light scattering measurement performed on octyl cyanobiphenyl (8CB) [17].

With the material parameters ξ_0, T_{NA}, and ν in hand, we fitted the theoretical form $\Psi=[(1+2\Omega)/(1+\Omega)]^{1/2}-1$ to our experimental values of Ψ, where Ω is derived in Ref. [7]

as $\Omega \approx 2(D_0/K_3 l)\int_0^\infty \sigma^2(z) z^2 dz$. The smectic order parameter profile $\sigma(z)$ is a function of $\xi(t)$, an interaction parameter r_0, and the quartic coefficient C^* in the free energy expansion for the bulk smectic order [7]; the parameters r_0, C^*, and D_0 were treated as fitting parameters. The line in Fig. 2 represents the fit, where the three fitting parameters are $D_0 = (3.5 \pm 0.9) \times 10^7$ erg/cm^3, $r_0 = (3.5 \pm 0.1) \times 10^6$ cm^{-1}, and $C^* = (3.0 \pm 0.3) \times 10^{12}$ cm^{-2}. The uncertainty in each of the parameters is based upon fits to the data [with the associated experimental error bars (see Fig. 2)], while holding all other parameters fixed. The value of D_0 obtained in our case is an order of magnitude greater than that for 8CB [6], although it should be noted that $D(z)$ scales *approximately* as D_0/C^*. Therefore, a similar fit could be obtained with a concomitant decrease in both parameters, which also would imply a larger surface-induced order parameter for SCE12R than for 8CB in Ref. [6]. It is difficult to make any comparisons for r_0, as there is no direct information available about the interaction between the liquid crystal molecules and the HTAB-coated substrate surface. We see that the theoretical curve plotted for these values of the fitting parameters qualitatively follows the general trend of the experimental data. Nevertheless, we also see that Ψ rises less sharply with decreasing temperature than does the correlation length (which corresponds to K_{33}), and that Ψ is not insignificant even 10 °C above T_{NA}. (This is in contrast to the results for the material 8CB in Ref. [6], where Ψ scaled as ξ more closely). One possible reason for this difference is the apparent temperature-dependent stiffness of SCE12R against tilt distortions, which could come about because of a large surface-induced smectic order parameter $\sigma(z)$, even well above T_{NA}. The effect of this stiffening would be that SCE12R, as compared to 8CB, would exhibit larger values of Ψ at comparable values of t over the entire nematic region; indeed, this is observed. Another possible complication is that flat regions exist between the grooves, and these regions are larger than the smectic correlation length. Therefore, we speculate that the smectic layering in the flat portion of the grooved regions may not be completely disrupted. (Due to experimental limitations, the flat regions between the grooves could not be avoided.) Additionally, from a theoretical standpoint there could also be a contribution from cross terms in the elastic deformation energy if we were to account for the variation of the surface-induced smectic order parameter in the layer plane. In this case, the one-dimensional problem considered in the analysis would be insufficient, and a considerably more complicated two-dimensional analysis would be needed. Finally, the simple model presented herein does not account for electric field imhomogeneities that occur at the grooved interface. Thus, despite the rough agreement between theory and experiment, a more detailed consideration of the actual surface topography, depth profile of K_{33}, and electric field profile must eventually be included in the theory.

In summary, our experimental results demonstrate that surface corrugations significantly disrupt the interfacial smectic order, with deeper and more closely spaced grooves having a larger disruptive influence. Although part of the discrepancy between theory and experiment may be due to experimental error, a more detailed theoretical analysis is required. These considerations will form part of our future work.

This work was supported by the National Science Foundation's Advanced Liquid Crystalline Optical Materials Science and Technology Center under Grant No. DMR89-20147 and by the U.S. Department of Energy under Grant No. DE-FG02-01ER45934. Acknowledgment is also made to the Donors of the Petroleum Research Fund, administered by the American Chemical Society, for partial support of this research under Grant No. 33983-AC5

[1] B. Jerome, Rep. Prog. Phys. **54**, 391 (1991).
[2] B. M. Ocko, A. Braslau, P. S. Pershan, J. Als-Nielsen, and M. Deutsch, Phys. Rev. Lett. **57**, 94 (1986).
[3] B. M. Ocko, Phys. Rev. Lett. **64**, 2160 (1990).
[4] J. Als-Nielsen, F. Christensen, and P. S. Pershan, Phys. Rev. Lett. **48**, 1107 (1982).
[5] E. A. L. Mol, G. C. L. Wong, J. M. Petit, F. Rieutord, and W. H. de Jeu, Physica B **248**, 191 (1998).
[6] C. Rosenblatt, Phys. Rev. Lett. **53**, 791 (1984).
[7] L. V. Mirantsev, Phys. Rev. E **59**, 5549 (1999).
[8] L. V. Mirantsev, Mol. Cryst. Liq. Cryst. Sci. Technol., Sect. A **301**, 137 (1997).
[9] C. Rosenblatt, J. Phys. (Paris) **45**, 1087 (1984).
[10] H. L. Ong, Phys. Rev. A **28**, 2393 (1983).
[11] A. J. Karn, S. M. Arakelian, Y. R. Shen, and H. L. Ong, Phys. Rev. Lett. **57**, 448 (1986).
[12] E. Santamato, G. Abbate, R. Calaselice, P. Maddalena, and A. Sasso, Phys. Rev. A **37**, 1375 (1988).
[13] S.-H. Chen and J. J. Wu, Appl. Phys. Lett. **52**, 1998 (1988).
[14] J. Shi and H. Yue, Phys. Rev. E **62**, 689 (2000).
[15] P. G. de Gennes, Solid State Commun. **10**, 753 (1972).
[16] C. W. Garland, M. Meichle, B. M. Ocko, A. R. Kortan, C. R. Safinya, L. J. Yu, J. D. Litster, and R. J. Birgeneau, Phys. Rev. A **27**, 3234 (1983).
[17] D. Davidov, C. R. Safinya, M. Kaplan, S. S. Dana, R. Schaetzing, R. J. Birgeneau, and J. D. Litster, Phys. Rev. B **19**, 1657 (1979).